Int. J. Dev. Biol. 53: 1457-1467 (2009)
doi: 10.1387/ijdb.072366mt

THE INTERNATIONAL JOURNAL OF DEVELOPMENTAL BIOLOGY
www.intjdevbiol.com

In vivo forced expression of myocardin in ventricular myocardium transiently impairs systolic performance in early neonatal pig heart

MARIO TORRADO[1], ALBERTO CENTENO[2], EDUARDO LÓPEZ[2] and ALEXANDER T. MIKHAILOV[1,*]

[1]Developmental Biology Group, Institute of Health Sciences, University of La Coruña and
[2]Experimental Surgery Unit, University Hospital "Juan Canalejo", La Coruña, Spain

ABSTRACT The aim of this study was to determine the effects of forced expression of *myocd-A* in the left ventricular (LV) myocardium on cardiac performance in early neonatal piglets. LV transfection with the gene for homeodomain only protein *(hop)*, an antagonist of *myocd*-mediated activities, was also performed. Gene delivery was performed in 6-day-old piglets using a low-traumatic, catheter-based, video-assisted procedure developed by us for direct intramyocardial injections of plasmid DNA into 3-4 target areas of the ventral LV free wall (LVFW). Two isoforms of porcine *myocd* were identified, cloned and characterized: the exon 11-lacking *myocd-A* and its larger exon 11-containig variant, *myocd-B*. In neonatal piglets, *myocd-A* seems to be a cardio-predominant isoform enriched in the LVFW/septum, whereas the *myocd-B* isoform is detected not only in the heart but also in various smooth muscle cell-containing tissues. Intramyocardial *myocd-A* gene delivery resulted in forced transgene expression in the target areas of the LVFW as compared to controls. On day 2 post-delivery, a marked decrease of LV-end systolic pressure values (an accepted marker for impaired LV function) was observed in *myocd-A*-transfected piglets as compared to *hop*-transfected and control groups. In addition, forced *myocd-A* expression in the LVFW caused abnormal ECG. A significant up-regulation of the gene for fetal-predominant muscle light chain 3F myosin was detected in *myocd-A*-transfected LVFWs harvested on day 2 post-delivery. Extended analysis on day 7 post-delivery revealed a drop decrease in *myocd-A* transgene expression in target LVFW regions which was correlated with normalization of the LV systolic parameters in experimented piglets.

KEY WORDS: *myocardin, gene delivery, myocardium, transcription factor, cardiac hypertrophy*

"The heart is the first organ to form and function in the embryo, and all subsequent events in the life of the organism depend on the heart's ability to match its output with the organism's demands for oxygen and nutrients"

(Olson, 2004).

Introduction

Myocardin *(myocd)* is a cardiac and smooth muscle-selective co-activator for the ubiquitous transcriptional factor, serum response factor (SRF). In the course of embryonic development, the onset of *myocd* expression coincides with specification of early cardiac progenitors in the cardiac crescent. Thereafter, *myocd* is expressed throughout the heart and in various subsets of smooth muscle cells (SMCs) (Creemers *et al.*, 2006a).

In *Xenopus* embryos, expression of a dominant-negative mutant of *myocd* (Wang *et al.*, 2001) or inhibition of *myocd* activity by morpholino knockdowns (Small *et al.*, 2005) disrupts cardiac development and abolishes cardiac marker gene expression. However, mouse embryos lacking *myocd* have a normal heart (Li

Abbreviations used in this paper: ANF, atrial natriuretic factor; EDP, end-diastolic pressure; ESP, end-systolic pressure; Hop, homeodomain only protein; LV, left ventricular; LVFW, LV free wall; myocd, myocardin; qRT-PCR, quantitative real-time RT-PCR; RV, right ventricular; SMC, smooth muscle cell; SRF, serum response factor; MLC3F, myosin light chain 3F isoform; CNN1, smooth muscle calponin 1 basic isoform; TAGLN, transgelin (SM-22); ACTG2, smooth muscle actin gamma 2 isoform; Q, poly(Q)-rich tract; SAP, SAF-A/B, Acinus and PIAS motif; TAD, transactivation domain; aa, amino acid residues; EtBr, ethidium bromide.

***Address correspondence to:** Dr. Alexander T. Mikhailov. Developmental Biology Group, Institute of Health Sciences. University of La Coruña. Campus de Oza, Building "El Fortín", As Xubias s/n. 15006 La Coruña, Spain. Fax: + 34-981-138-714. e-mail: margot@udc.es

Final author-corrected PDF published online: 30th January 2008.

ISSN: Online 1696-3547, Print 0214-6282

et al., 2003) probably due to redundancy of *myocd*-related factors (Wang *et al.*, 2002), which are expressed in the developing mouse, but not in the developing *Xenopus* heart (Small *et al.*, 2005). Recently, it was found that *myocd* is transiently expressed within the somites of mouse embryos. However, forced *myocd* expression in *in vitro* cultured skeletal myoblasts resulted in repression of activity of the muscle-specific myogenic factors and concurrent activation of SMC-specific genes (Long *et al.*, 2007).

It is widely accepted that *myocd* is a regulatory factor that plays pivotal roles in both cardiac and SMC gene expression (recently reviewed in: Liu and Olson, 2006; Pipes *et al.*, 2006; Parmacek, 2007). In *Xenopus* embryos, ectopic *myocd* expression results in activation of cardiac muscle genes throughout the embryo, including spinal cord neurons (Wang *et al.*, 2003), or in animal cap tissue (Small *et al.*, 2005). In cultured mammalian cells, depending on the particular cell type in which *myocd* expression is induced, different subsets of SRF-dependent SMC and cardiac muscle genes can be activated (Chen *et al.*, 2002b; Du *et al.*, 2003; Wang *et al.*, 2003; Yoshida *et al.*, 2003; Hendrix *et al.*, 2005; Pipes *et al.*, 2005; van Tuyn *et al.*, 2005, 2007a,b; Creemers *et al.*, 2006a,b; Chow *et al.*, 2007).

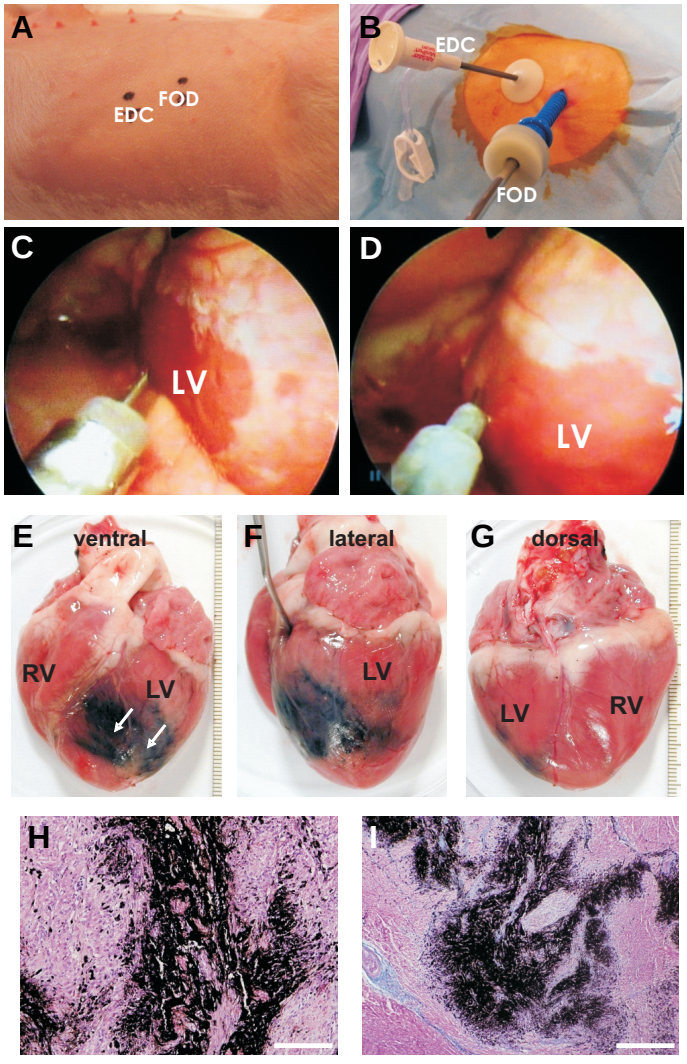

Fig. 1. Procedure of catheter-based video-assisted intramyocardial injections of Indian ink suspension into the left ventricular free wall (LVFW) of 6-day-old piglets. (A) *Positions for trans-cutaneous insertion of the endoscopic cannula (EDC) and fiber-optic device (FOD) into left chest cavity. The positions were selected to access and visualize the ventral surface of the heart.* **(B)** *Both EDC and FOD are inserted at the positions indicated.* **(C,D)** *Intramyocardial injecting controlled by real-time video-signals. LV, left ventricle.* **(E,F,G)** *Ventral, lateral and dorsal view of the heart at the 7th day after Indian ink delivery to the ventral LVFW. Arrows, injection points; RV, right ventricle.* **(H,I)** *Histological sections showing Indian ink infiltration of the myocardium at injection points. Haematoxylin-eosin staining. Bar, 100 μm.*

However, although *myocd* is required for cardiac and SMC gene expression and differentiation, it is not sufficient to cause other cell types to adopt a cardiac or SMC expression phenotype (Yoshida *et al.*, 2004). In this regard, *myocd* can initiate the expression of cardiac muscle-specified genes in cultured fibroblasts, but only in the presence of the co-expressed small ubiquitin-like modifier, SUMO-1 (Wang *et al.*, 2007). Undifferentiated liver-derived stem cells acquire a cardiomyocyte phenotype when co-cultivated *in vitro* with neonatal cardiomyocytes which, in turn, results in the *de novo* activation of cardiac transcriptional factors including *myocd* (Muller-Borer *et al.*, 2007). These and other data (Oh *et al.*, 2004; Callis *et al.*, 2005; Creemers *et al.*, 2006a) strongly suggest that additional factors are required to promote myocardin's role in cardiogenic gene expression.

In addition to its roles in the regulation of cardiac and SMC differentiation and gene expression, *myocd* has also been implicated in remodeling of the postnatal heart in response to either physiological or pathological stresses during heart ageing, cardiomyopathic progression, and at heart failure (see Table 1 and references therein). Physiological and experimental cardiac hypertrophy is accompanied by marked *myocd* up-regulation in ventricular myocardium. In this regard, *in vitro* forced expression of *myocd* in neonatal ventricular cardiomyocytes increases cell size and expression of molecular markers of cardiac hypertrophy (Badorff *et al.*, 2005; Xing *et al.*, 2006). Glycogen synthase kinase 3β, suppressor of cardiomyocyte hypertrophy (Michael *et al.*, 2004), phosphorylates MYOCD, thus antagonizing its pro-hypertrophic activity (Badorff *et al.*, 2005).

Taken together, these studies all point to a redeployment of *myocd* in processes of postnatal cardiac remodeling (Torrado *et al.*, 2003; Torrado *et al.*, 2005a; Oka *et al.*, 2007). While some potential insights into MYOCD/SRF-dependent pathways were described in cultured neonatal cardiomyocytes, the functional contributions of *myocd* signaling to physiological cardiac hypertrophy in the neonatal heart *in vivo* remain unknown.

The primary goal of the present study was to directly assess the possible roles of MYOCD in the neonatal porcine heart *in vivo*. To this end, a new controlled local delivery of *myocd-A*-expressed plasmids to left ventricular (LV) myocardium was developed. Using this low traumatic technique, the effects of transfection-mediated *myocd-A* overexpression in the LV myocardium on cardiac performance and gene expression were monitored in neonatal pig hearts. As additional experimental treatments, LV transfection with the gene for homeodomain only protein (*hop*), an antagonist of *myocd*-mediated SRF activities (Kook and Epstein, 2003), was also performed.

Here we show that *in vivo* forced expression of *myocd-A* in ventricular myocardium transiently impairs systolic performance in neonatal pig hearts. Given that end-stage heart failure is

accompanied by an increase in *myocd* expression (see Table 1), these results demonstrate, for the first time, that myocardial *myocd* overexpression might represent a maladaptive response to cardiac stress.

Results

The use of a newly developed catheter-based device results in efficient intramyocardial delivery in closed-chest neonatal piglets

Direct intramyocardial delivery is attractive because specific myocardial regions can be targeted and high local concentrations of the transgene can be achieved. However, direct myocardial gene delivery often requires aggressive surgical interventions resulting in a low survival rate of experimental animals.

We developed and evaluated the feasibility of a catheter-based video-assisted surgical approach for direct intramyocardial gene transfer in closed-chest 6-day-old neonatal piglets (Fig. 1A-D). For catheter optimization studies, needle length (2-5 mm), injection volume (50-200 μl/point), and the localization/distribution of the delivered trackers (Indian ink suspension or β-galactosidase (β-gal) carrying plasmid DNA) were assessed two and seven days after injections.

The intramyocardial injections were well tolerated in all animals. Sometimes, injections provoked isolated ventricular ectopic beats but no sustained dysrhythmia. In all delivery experiments, piglets became fully ambulatory during the first 30 min after removal of anesthetics. Histological analysis revealed no evidence of inflammatory cell infiltration or micro-infarctions in LVFW regions injected with naked β-gal plasmid DNA at the 7th day post-delivery. However, injections of the β-gal plasmid DNA solution supplemented by *in vivo*-jetPEI transfection reagent (at N/P=10) did result in signs of inflammation and calcium deposition in the targeted LVFW regions.

The optimal needle length in these neonatal piglets with a LVFW thickness of 7.3± 0,3 mm (Torrado *et al.*, 2004) was determined to be 4 mm and, using this needle length, the optimal injection volume was determined to be 100 μl/point. Under our conditions, 3-4 discrete injections (100-150 μl each), spaced 1 cm apart, in each LVFW resulted in distribution of Indian ink tracker across ~50% of the ventral LVFW surface (Fig. 1E).

Furthermore, to determine more precise quantitative data regarding transfection efficiency, myocardial delivery of β-gal plasmid DNA was performed using the same injection protocol. Protein extracted from injected and adjacent regions of each LVFW was assayed for β–gal enzymatic activity. The same or an even more vast distribution of β-gal enzymatic activity was found in the corresponding LVFWs as compared to that in myocardium injected with Indian ink suspension. These results were further confirmed by reverse transcription-polymerase chain reaction (RT-PCR) detection of β–gal expression in the injected LVFW regions (data not shown).

In conclusion, the use of the optimized intramyocardial delivery device with video-assisted guidance resulted in a relatively efficient delivery of the trackers used to target the regions of the LVFW with 100% recovery of experimental piglets.

Which porcine myocardin *gene to use for delivery?*

Previously, we have provided evidence for the existence of two *myocd* transcript variants in four cardiac cambers, as well as in aorta, pulmonary vein, and lung of neonatal piglets (Torrado *et al.*, 2003). In this work, two porcine *myocd* variants were cloned, sequenced and designated, in accordance with our tentative classification (Torrado *et al.*, 2003), as a *myocd-A* and its spliced variant *myocd-B*, containing a 144-bp insertion due to the presence of an alternative exon (marked 11 in Fig. 2A and Fig. 4A).

Using RT-PCR, both *myocd-A* and *myocd-B* transcripts were detected in all heart chambers of 6-8-day-old neonatal piglets with relative *myocdA/myocd-B* expression ratio (fold expression) of 1:9±2.8 (Fig. 2B, C). *Myocd-B* was also found to be expressed in aorta, pulmonary veins, lung and spleen, but its expression was not detectable in skeletal muscle, liver and kidney. In contrast, in addition to being expressed in myocardium, *myocd-A* mRNA, was weakly detected only in aorta (Fig. 2C).

To confirm that each of the two *myocd* transcripts can be efficiently translated into protein, the corresponding myc/His-tagged cDNAs were expressed *in vitro* and the encoded polypeptides were detected by SDS-PAGE followed by Western blot with our lab-derived anti-CT-MYOCD-A (named AB531; see Fig. 4B, C) or anti-myc antibodies. On blots, both MYOCD-A and MYOCD-B proteins were detected by each of the antibodies used (Fig. 2D, E). The experimentally determined molecular weight (MW) value of myc/His-tagged MYOCD-A (128 kDa) and MYOCD-B (133 kDa) is an ~28 kDa higher than the predicted sequence-derived

TABLE 1

MYOCARDIN EXPRESSION LEVELS AT HEART AGING, VENTRICULAR HYPERTROPHY AND HEART FAILURE

Model	Cardiac phenotype	Phase/Clinical syndrome	Myocardin (up/down)	Reference
Young *vs* newborn piglets	VH due to early postnatal growth	Physiological VH	transcript (up)	Torrado *et al.*, 2003
Old *vs* young adult mice	Aging heart	NA	transcript (up)	Zhang *et al.*, 2004
Old *vs* young adult humans	Aging heart	NA	transcript (up)	Zhang *et al.*, 2004
Adult TAB mice	VH due to aortic stenosis	No signs of HF	transcript (up)	Xing *et al.*, 2006
Calcineirin-transgenic mice	VH due to calcineurin overexpression	Susceptible to sudden death	protein (up)	Xing *et al.*, 2006
SRF-deficient adult mice	DCM due to disruption of the SRF gene	Early-stage DCM	transcript (down)	Parlakian *et al.*, 2005
		End-stage HF	transcript (up)	
Dox-injected piglets	DCM due to Dox cardiotoxic effects	End-stage HF	transcript (up)	Torrado *et al.*, 2003
F *vs* NF human hearts	IDCM	End-stage HF	transcript (up)	Torrado *et al.*, 2003
F *vs* NF human hearts	IDCM	No signs of HF	protein (no change)	Xing *et al.*, 2006
	IDCM	End-stage HF	protein (up)	

VH, ventricular hypertrophy; NA, not available; TAB, thoracic aortic banding; HF, heart failure; SRF, serum response factor; DCM, dilated cardiomyopathy; IDCM, idiopathic DCM; Dox, doxorubicin; F, failing; NF, non-failing heart.

MW of porcine MYOCD-A (~101 kDa) and MYOCD-B (~105 kDa), respectively.

To the best of our knowledge differences in apparent *versus* deduced MW of MYOCD proteins have not been recognized in previous studies on mouse *myocd* (Creemers *et al.*, 2006b; Xing *et al.*, 2006; Wang *et al.*, 2004, 2007). On the other hand, one can deduce from published SDS-gel images (see Qiu *et al.,* 2005; Li *et al.,* 2007) that an apparent MW of FLAG-tagged mouse MYOCD seems to be between 120-130 kDa that is similar to the MW value of myc/His-tagged porcine MYOCD-A (this work). It seems that the presence of myc/His residues (see Fig. 2D,E) or FLAG epitopes (see Fig. 3B) in expressed MYOCD proteins contributes only to a minor extent to analomous slow migration of the pig MYOCD proteins in SDS-PAGE gels. Of note, the experimentally estimated 5-kDa difference between the myc/His-tagged 128-kDa MYOCD-A and the 133-kDa MYOCD-B closely agreed with the theoretical 4-kDa size difference between these two isoforms of porcine MYOCD (i.e., 101 kDa *vs* 105 kDa).

Furthermore, using AB531-antibodies, a single 145-kDa band was immuno-decorated on blots of electrophoresed SDS-lysates from LV but not from skeletal muscle of neonatal piglets (Fig. 2D). The specificity of this cross-reactivity was confirmed by pre-absorption of AB531 with the competing peptide, which blocked immuno-detection of the heart-derived 145-kDa band. Of note, the fragment 5 of pig *myocd-A* used as immunogen to generate AB531 antibodies (see Fig. 4B) is identical for both porcine *myocd-A* and *myocd-B* isoforms. Therefore, it was not surprising that these antibodies recognized both *in vitro* synthesized MYOCD-A and MYOCD-B proteins (see Fig. 2D). However, we observed the only one 145-kDa band on piglet LV-derived immunoblots (see Fig. 2D). Although unproved as yet, we suggest that the band with an apparent MW of 145-kDa might correspond to an endogenous MYOCD-B protein. In this respect, we found that the *myocd-B* mRNA is much more abundant than the *myocd-A* transcript in the LV (see Fig. 2 B,C) suggesting that under our experimental conditions presumably MYOCD-B protein might be detected on LV-derived blots. Differences in an apparent MW between *in vitro* expressed MYOCD-B (MW 133-kDa) and heart-derived protein (MW 145 kDa) may be due to post-translational modifications of the latter, such as symolation (Wang *et al.*, 2007), or due to its conformation changes. In this context, SUMO-modified transcription factors have a ~20 kDa higher apparent MW as compared to unmodified proteins (Eloranta and Hurst, 2002; Sapetschnig *et al.*, 2002).

Collectively, the results revealed a differential expression of *myocd-B versus myocd-A* genes in the piglet LV myocardium and a modest but steady level of *myocd-A.* In neonatal piglets, the exon 11-lacking *myocd-A* seems to be a cardiac-predomi-

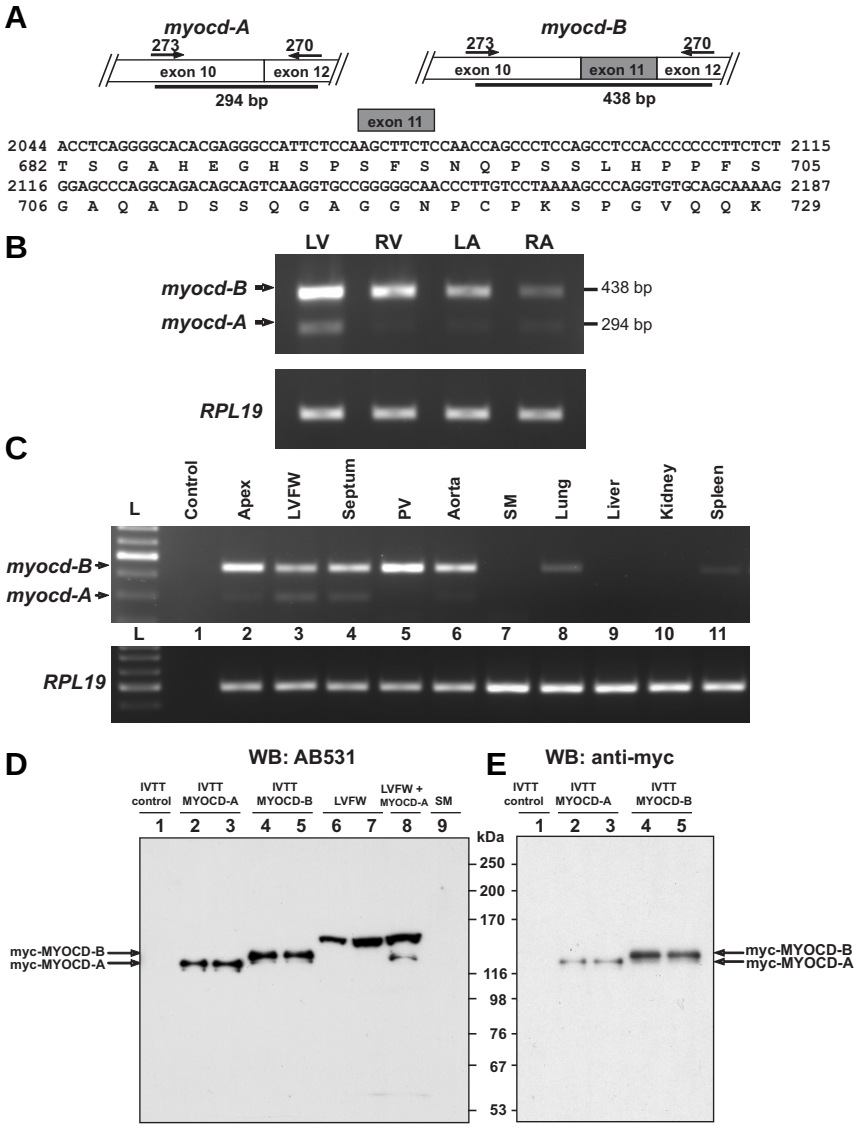

Fig. 2. Analysis of *myocd-A* and *myocd-B* expression *in vivo* and *in vitro*. (A) *Positions of the oligonucleotides 273 and 270 (horizontal arrows) over porcine* myocd-A *and* myocd-B *exon 10 and exon 12 (white boxes) that have been used in RT-PCR analysis. Spliced exon 11 in* myocd-B *is boxed in grey. Bold-faced black lines indicate 294-bp and 438-bp PCR fragment of the pig* myocd-A *and* myocd-B*, respectively (top part). Nucleotide and deduced amino acid sequences of the* myocd-B *exon 11 (lower part).* **(B)** *Representative semiquantitative RT-PCR for* myocd-A, myocd-B *and* RPL19 *genes in left and right ventricles (LV, RV) and atria (LA, RA) of 6-day-old piglets.* **(C)** *Expression of* myocd-A *and* myocd-B *in LV-derived tissues and various non-cardiac tissues/organs of 8-day-old piglets as determined by semiquantitative RT-PCR. PV, pulmonary vein; SM, skeletal muscle; L, DNA ladder; Control, non-template PCR.* **(D,E)** *Western blot analysis of* in vitro *(IVTT) expressed* myc-*tagged* myocd-A *(lane 2, 3) and* myocd-B *(lane 4, 5) cDNAs using anti-CT-MYOCD (AB531) and anti-myc antibodies, respectively. Lane 1 (IVTT control), non-plasmid DNA negative control. In addition, extracts prepared from LVFW of 8-day-old neonatal piglets were probed with anti-CT-MYOCD antibodies (right part of D): lane 6, LVFW extract (15 μg of total protein); lane 7, LVFW extract (30 μg of total protein); lane 8, IVTT-expressed* myocd-A *protein was loaded together with LVFW extract (LVFW+MYOCD-A); lane 9, extract from skeletal muscle (SM, 30 μg of total protein) of 8-day-old neonatal piglets.*

nant isoform enriched in LVFW and septum whereas the exon 11-containing *myocd-B* isoform is expressed not only in the heart but also in SMC-containing tissues such as aorta, pulmonary veins, lung and spleen (see Fig. 2 A-C). Of note, forced expression of similar (see Fig. 4A) human *myocd-A* and *myocd-B* isoforms in myocardial scar fibroblasts didn't reveal significant differences in their transactivating capacity, making the biological relevance of *myocd-B* exon 11 uncertain (Tuyn *et al.,* 2007b). Additionally, we reasoned that since the baseline levels of *myocd-A* expression are low in the piglet myocardium, the consequences of forced *myocd-A* expression in the LVFW could be more palpable than in case of *myocd-B* delivery. Given also that comparison of the effects and quantitative measurements of the delivered *myocd* variants could significantly interfere with endogenous *myocd* transcripts/proteins, for gene delivery experiments we used the *myocd-A*-carrying plasmid.

Intramyocardial delivery of myocardin-A *results in transiently impaired systolic performance*

Using the optimal delivery protocol developed in the first part of the work, naked plasmids encoding *myocd-A* gene, *hop* gene or vector itself were injected directly into target sites of the LVFW of 6-day-old neonatal piglets. Two days after delivery, nine regions of each injected LVFW (Fig. 3A) were assayed individually by Western blot with anti-FLAG-antibody (Fig. 3B) and RT-PCR (Fig. 3C,D). To ensure the specificity of RT-PCR for delivered cDNAs, we used RT-PCR with discriminating primer sets. In all RT-PCR experiments, we observed highly specific amplification of only the template specific for the discriminating downstream primer complementary to the FLAG-tagged *myocd-A* (Fig. 3C, D) or *hop* sequence (data will be described elsewhere).

All *myocd-A*-transfected LVFWs (n=10) harvested on day 2 post-delivery demonstrated transgene expression detectable by RT-PCR. The relatively high ectopic expression of the FLAG-*myocd-A* was restricted almost exclusively to segments 3, 5, and 6 that included the injection sites. FLAG-*myocd-A* transgene expression was not found in other tissue segments except in the two LWFWs, which also revealed transgene expression in region 2 and 4 (Fig. 3C). The results of non-RT control PCR runs demonstrated that the FLAG-*myocd-A* PCR product was amplified from LV cDNA, but not from plasmid DNA (see Fig. 3D). On average, the estimated extent of FLAG-*myocd-A* expression was 40% of the overall area of the ventral LVFW. Target delivery regions of LVFWs (i.e., region 3, 5, and 6) injected with *hop* or empty vector were consistently negative for FLAG-*myocd-A* transgene expression (data not shown).

The *myocd-A/myocd-B* mRNA ratio in FLAG-*myocd-A*-delivered LVFW regions was significantly affected as compared to that in myocardium of PBS-

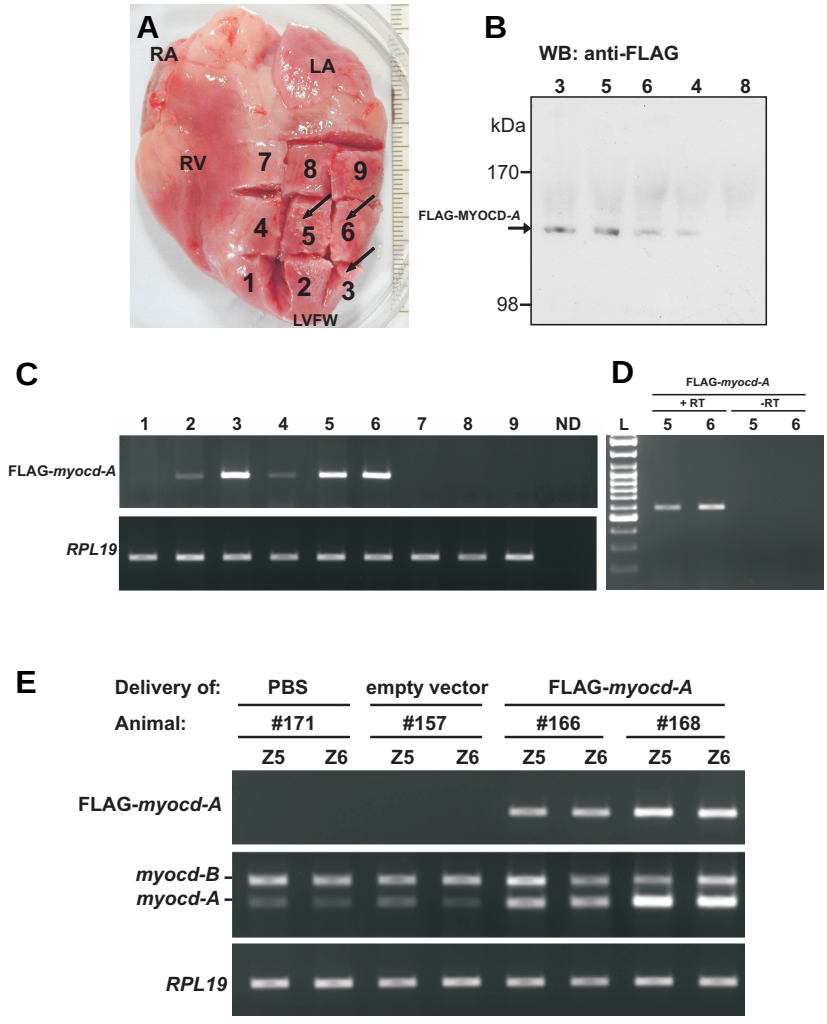

Fig. 3. Representative analysis of FLAG-tagged *myocd-A* expression in the left ventricular free wall (LVFW) myocardium 48 h after gene delivery (8-day-old piglets). (A) myocd-A *transfected LVFW (arrows, injection positions) was dissected into nine fragments (1-9). RV, right ventricle; RA and LA, right and left atrium, respectively.* **(B)** *Western blot detection of FLAG-tagged MYOCD-A protein in dissected target (3, 5, 6) and adjacent (4, 8) regions of* myocd-A *transfected LVFW.* **(C)** *Semiquantitative RT-PCR analysis of FLAG-tagged* myocd-A *transcript levels in nine LVFW segments (after normalization of the cDNA templates to* RPL19 *expression). ND, non-delivered myocardium.* **(D)** *Control of plasmid DNA contamination in RNA preparations used in downstream RT-PCR assays (see C,E). Total RNA was isolated from the target regions 5 and 6 of* myocd-A *transfected LVFW (see A). Four μg of each RNA preparation were reverse transcribed (RT) in 20 μl reaction mix. One μl of each RT reaction (+RT) and 1 μg of each RNA (-RT) were subsequently used in a standard PCR reaction for the amplification of the FLAG-tagged* myocd-A *message. Equal volumes of each PCR reaction were assessed on a 2% agarose gel and stained with EtBr. L, GeneRuler DNA ladder mix (Fermentas).* **(E)** *Semiquantitative RT-PCR analysis of total RNAs isolated from the indicated zones (Z5, Z6) of LVFWs injected with PBS (piglet #171), empty vector (piglet #157) or FLAG-tagged* myocd-A *(piglet #166 and #168) plasmids. Upper part, recombinant FLAG-*myocd-A *transcript levels. Middle part, endogenous/recombinant* myocd-A *and endogeneous* myocd-B *transcript levels. Lower part,* RPL19 *transcript levels.*

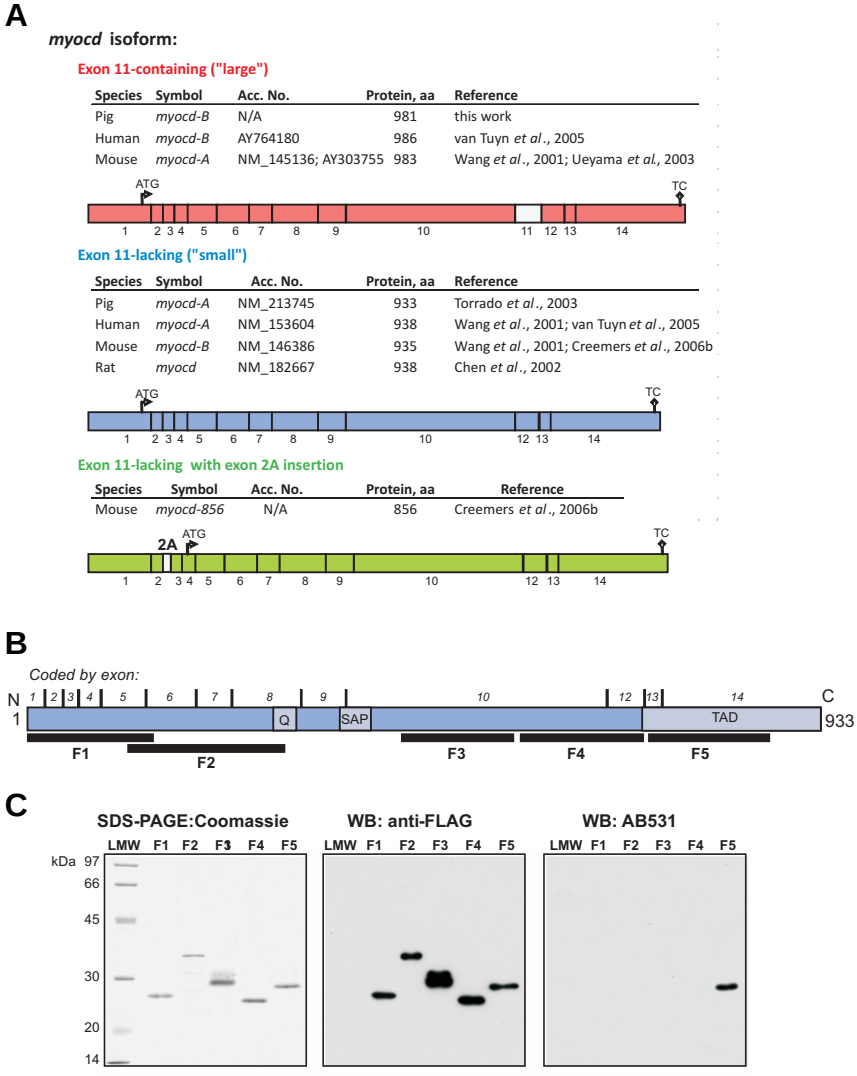

Fig. 4. Alternative splicing yields different *myocd* transcripts with similar C-termini coded by exons 13 and 14. (A) *Schematic diagrams of three different* myocd *isoforms (marked respectively in red, blue and green) detected in cardiac and SMC-containing tissues.* Myocd*, gene name approved by HUGO Gene Nomenclature Committee. Transcript symbols are indicated in accordance with original definitions. 1-14, exons (alternative exon 2A and 11 are boxed in white). In each* myocd *isoform, the transactivation domain is coded by similar exons 13 and 14. The exon 11-lacking* myocd A *(blue) and exon 11-containing* myocd-B *(red) have similar N-terminal peptide sequences. Green, N-terminus truncated* myocd *isoform. ATG and TC, translation initiation and termination codon, respectively. aa, amino acid residues. N/A, not available.* **(B)** *Five fragments (F1-5 marked by bold-faced black lines) covering the major part of the sequence of porcine MYOCD-A were cloned, expressed and purified as described in Materials and Methods. The C-terminal (CT) fragment 5 of porcine MYOCD-A (aa 731-873) was used, as immunogen, to generate AB531 antibodies. Q, poly(Q)-rich tract. SAP, SAF-A/B, Acinus and PIAS motif. TAD, transactivation domain.* **(C)** *Purified fragment products (F1-5) were separated by SDS-PAGE followed by Coomassie staining of gels (left) or Western blot (WB) with anti-FLAG (center) and AB531 antibodies (right). Anti-FLAG antibodies detect all fragments due to presence of the FLAG epitopes in each expressed protein. AB531 antibodies recognize only the CT fragment 5 used for immunization; no cross-reactively was observed with other MYOCD-A-derived fragments. LMW, Amersham low molecular weight calibration kit.*

and vector-delivered (Fig. 3E) or age-matched (Fig. 2B,C) piglets. In the target regions, delivered FLAG-*myocd-A* caused an increase of the *myocd-A* transcript content in direct proportion to the transgene expression level. The amount of the endogenous *myocd-B* RNA did not change appreciably in *myocd-A*-delivered regions (Fig. 3E). Of note, intramyocardial delivery of the vector itself did not influence endogenous *myocd-A/myocd-B* mRNA levels in the target regions of LVFWs. Histological examination did not reveal inflammation or fibrosis in the LVFW target regions from *myocd-A*- delivered piglets (data not shown).

Ventricular systolic function was clearly altered in *myocd-A*-delivered piglets as compared with that in animals intramyocardially injected with *hop*-plasmid or the vector itself. Particularly, intramyocardial injections of *myocd-A* resulted in a marked decrease of LVESP, an accepted marker for impaired LV function. In addition, forced *myocd-A* expression in the LVFW caused abnormal ECG including T-wave inversion (Table 2). In *hop*-delivered and control groups, there was no change in ECG parameters from gene delivery to final studies, nor were there differences in LVESP values between these groups.

In all animals, LVEDP (a marker for LV compliance) values were the same regardless of whether *myocd-A* or other plasmids were delivered into myocardium. In *myocd-A* delivered hearts, there was no difference in the heart mass as assessed by the ratios of heart/body weight compared with control piglets (Table 2).

To examine the duration of expression from the delivered *myocd-A* naked DNA, we have analyzed by RT-PCR the level of FLAG-*myocd-A* mRNA in hearts (n=5) harvested after 7 days after gene delivery. On day 7, the transgene expression level in the LV target regions was, on average, 3-fold less than that on day 2. The systolic parameters were not altered in this animal group as compared to age-matched controls (i.e., 13-day-old piglets; n=4) transfected with empty vector (data not shown). These experiments show the transient character of *myocd-A* transgene expression in the heart and strongly suggest that only a highly forced *myocd-A* expression might have a functional consequences on LV systolic performance.

Considering the well-established involvement of *myocd* in regulating both cardiac and SMC gene expression, we studied in *myocd-A*-delivered hearts the endogenous expression of a set of the genes previously shown to be *bona fide myocd* targets. Expression of selected cardiac and SMC marker genes was assessed by qRT-PCR in FLAG-*myocd-A*- (n=5) *versus* vector-delivered (n=4) piglets two days after transfection (Table 3; Fig. 5). These gene expression studies were performed using myocardial samples derived from two target region 5 and 6 (see Fig. 3A) of each LVFW transfected with *myocd-A* (5 animals) or empty vector

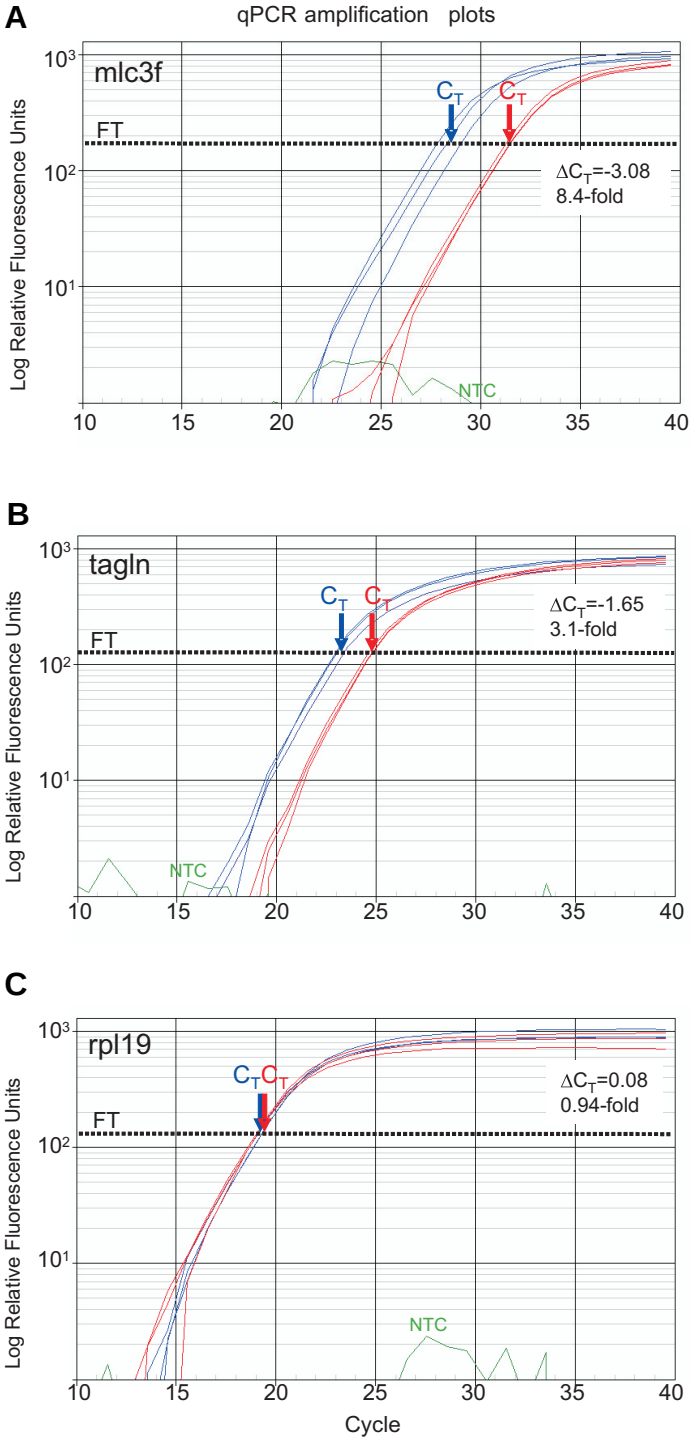

Fig. 5. Representative qRT-PCR analysis of *mlc3f* (A) and *tagln* (B) expression levels in *myocd-A versus* vector-transfected left ventricular (LV) myocardium two days after delivery. *For each gene, mRNA levels (normalized to* **(C)** *the internal standard* rpl19*) were measured in six samples, each derived from the target region 5 (see Fig. 3A) of three* myocd-A- *(blue plots) and three empty vector-injected (red plots) LVFWs. C_T, cycle threshold; ΔC_T, differences in threshold cycles for target and reference. Calculated fold-change in* mlc3f *and* tagln *expression levels is shown. FT, fluorescence threshold. NTC (green), non template control.*

(4 animals). In total, 10 FLAG-*myocd-A*- and 8 vector-delivered samples were processed. The gene for myosin light chain 3F (*mlc3f*) displayed the most remarkable, over 8-fold up-regulation in response to intramyocardial *myocd-A* delivery (Fig. 5A; Table 3). Of note, we didn't detect expression of the spliced *mlc1f* isoform in the neonatal myocardium of 8-day-old control and *myocd-A* transfected piglets. Among the studied SMC marker genes, only *trangelin/SM-22* (*tagln*) was markedly and statistically significantly stimulated in response to FLAG-*myocd-A* (Fig. 5B, Table 3). The expression levels of the gene for atrial natriuretic factor (*anf*), smooth muscle calponin 1 (*cnn1*) and smooth muscle actin gamma 2 (*actg2*) were also up-regulated in the *myocd-A*-delivered LVFW regions as compared to those injected with the vector itself, but the differences were not statistically significant.

Collectively, the results indicate that under our experimental conditions *myocd-A*-delivered hearts shown signs of transiently impaired systolic function that is associated with marked activation of *mcl3f* and *tagln* expression in target LVFW regions on day 2 post-delivery.

Discussion

The recent discovery of MYOCD that modulates the activities of SRF in cardiac and SMC tissues (Wang *et al.*, 2001) has led to intensive investigation into the role that MYOCD can play in heart development and disease and has revealed new combinatory pathways by which MYOCD can regulate cardiac gene expres-

TABLE 2

CARDIAC PARAMETERS OF NEONATAL PIGLETS INTRAMYOCARDIALLY INJECTED WITH *MYOCD-A*, *HOP*, *β-GAL*, AND PLACEBO PLASMIDS ON DAY 2 POST-DELIVERY

Parameter	*myocd-A*	*hop*	β-*gal*	Vector itself
Number of animals	10	6	6	4
Heart to body weight ratio, x1000	6.5±0.3	6.9±0.3	7.4±0.4	6.5±0.2
Heart rate (beats/min)	163±35	161±40	174±31	140±16
LV end-systolic pressure (mm Hg)	37.2±3.2*	62.2±4.2	61.8±3.1	61.0±3.3
LV end-diastolic pressure (mm Hg)	4.6±1.4	5.6±1.4	4.3±1.3	5.5±1.2
T-wave ischemic changes, %	20	0	0	0

* p< 0.05

TABLE 3

RESPONSES OF CARDIAC AND SMC MARKER GENES TO FORCED *MYOCD-A* EXPRESSION IN LVFW TARGET REGIONS ON DAY 2 POST-DELIVERY

Gene	Acc. No.	Fold change mean ± SEM	*myocd* target / reference
mlc3f	DQ629159	8.1±1.5 *	cardiac / Creemers *et al.*, 2006b
anf	NM_214260	1.2±0.2	cardiac / Xing *et al.*, 2006
cnn1	NM_213878	1.3±0.2	SMC / Chen *et al.*, 2002b
tagln	AK234135	2.9±0.3 *	SMC / Yoshida *et al.*, 2003
actg2	AK240464	1.4±0.2	SMC / Pipes *et al.*, 2005

qRT-PCR analysis of mRNA levels of target genes (normalized to the internal standard *rpl19*) in FLAG-*myocd-A* delivered LVFW regions (sample size=10, see text). Fold change as compared to LVFW regions injected with empty vector. References – bibliographic information used for our selection of the genes as the direct *myocd* targets. *mlc3f*, myosin light chain 3f isoform; *anf*, atrial natriuretic factor gene; *cnn1*, smooth muscle calponin 1 basic isoform; *tagln*, transgelin (SM-22); *actg2*, smooth muscle actin gamma 2 isoform. * p< 0.05.

sion (reviewed in: Liu and Olson, 2006; Pipes *et al.*, 2006; Parmacek, 2007). However, consequences of MYOCD up-regulation during physiological and pathological LV remodeling in the postnatal heart *in vivo* (see Table 1) have not yet been highlighted. In this study, we present the results of the first step of our approach to determining whether MYOCD up-regulation in the LV of neonatal piglets might have functionally significant consequences.

As previously reported, mouse (Wang *et al.*, 2003), human (Du *et al.*, 2003; van Tuyn *et al.*, 2005) and pig (Torrado *et al.*, 2003) *myocd* gene can undergo alternative splicing in cardiac and SMC-containing tissues. Our *in silico* analysis (Fig. 4A) of the *myocd* gene transcript variants identified in human, pig, rat and mouse cardiac and SMC-containing tissues shows that: (1) differential splicing does give rise to, at least, three different *myocd* transcripts: *myocd-A*, *myocd-B*, and N-terminus truncated isoform, (2) both *myocd-A* (i.e., the exon 11-lacking isoform) and *myocd-B* (i.e., the exon 11-containing isoform) initiate translation at the ATG codon located in exon 1 producing a MYOCD-A "small" (933-938 aa) and MYOCD-B "large" (981-986 aa) protein, respectively, and (3) alternative splicing of exon 2 to exon 2a, introduces a stop codon in exon 1 so that translation is initiated from the additional ATG codon located in exon 4 generating the 856 aa protein variant. Excepting this N-terminus truncated isoform, all *myocd-A/B* alternative variants contain the domains required for interactions with SRF and myocyte-specific enhancer factor 2 (MEF2), as well as, the transactivation domain. The N-terminus truncated isoform lacks the sequence required for interaction with MEF2 (Creemers *et al.,* 2006b).

In this work, two forms of the porcine *myocd* were identified, cloned and characterized (see Fig. 2 and Fig. 4A): *myocd-A* and its larger splice variant, *myocd B*. Both isoforms of porcine *myocd* are expressed in cardiac chambers of the neonatal pig heart with much lower levels of the *myocd-A* transcript as compared to those of the *myocd-B*. These results are consistent with the data on expression patterns of the similar *myocd-A* and *myocd-B* transcripts in human heart (van Tuyn *et al.,* 2005) but differ from those in mouse. In mouse, the *myocd-B* isoform (encoded a 935-aa protein) was detected by RT-PCR predominantly in the heart, whereas the N-terminus truncated *myocd* isoform (encoded a 856-aa protein), in aorta (Creemers *et al.,* 2006b). In this light, in neonatal piglets the *myocd-A* "small" isoform enriched in LV and ventricular septum seems to be a cardiac-predominant isoform, whereas the *myocd-B* "large" variant is expressed at comparable levels not only in the heart but also in aorta and pulmonary veins (see Fig. 2 B,C).

Comparison of the human isoforms of *myocd* (that are similar to porcine *myocd-A* and *myocd-B*; see Fig. 4A) failed to detect differences in their transactivating capacity (van Tuyn *et al.*, 2005, 2007b). The present study demonstrates that one-time direct intra-myocardial administration of naked plasmid encoding the porcine *myocd-A* results in the sustained expression of the delivered gene in the target regions of the piglet LVFW on day 2 post- delivery. In turn, this forced *myocd-A* expression in the LV myocardium results in impaired systolic function. Notably, LVFW delivery of the *hop* gene that can diminish the cooperativity between MYOCD and SRF (Chen *et al.*, 2002a; Shin *et al.*, 2002) or empty vector did not result in altered ventricular performance. FLAG-tagged *myocd-A* expression was significantly downregulated in target LV regions 7 days after delivery that coincided with full recovery of LV systolic performance in experimented piglets.

In fact, we demonstrated that the injection of naked *myocd-A* DNA, whose high transgene expression could be detected within first several days post-delivery, was enough to trigger a transient LV systolic dysfunction. How can this effect be explained? Impaired LV performance might have been most easily rationalized by forced expression of the *myocd-A* isoform, the level of which is much lower in normal piglet (this work) and human (van Tuyn *et al.*, 2005) LV myocardium in comparison to levels of the spliced *myocd-B* isoform. Thus, one possibility is that selectively altered expression of the *myocd-A* over baseline may be non-physiological for rapid postnatal remodeling of the LV myocardium. In this sense, we detected a significant *mcl3f* up-regulation in neonatal porcine myocardium in response to *myocd-A* delivery (see Table 3, Fig. 5A). Although *mcl3f* expression was previously thought to be restricted to fast skeletal muscles, later the gene was found to be also expressed in developing mouse heart. Its expression is down-regulated after birth and no traces of the MLC3F protein was detected in adult mouse heart (Kelly *et al.*, 1995; 1998; McGrew *et al.*, 1996). It is formally possible that overexpression of the fetal-predominant MLC3F fast myosin isoform in neonatal LV-myocardium in response to *myocd-A* delivery might interfere with other MLC proteins altering, in turn, the contractile performance of growing piglet myocardium. We cannot also discount the possibility that in porcine neonatal myocardium the *myocd-A*/*myocd-B* ratio might act as a "dimmer switch" to fine-tune expression levels of a set of SRF-dependent genes. In this sense, the shifting of the *myocd-A/myocd-B* ratio in *myocd-A*-delivered LVFW regions in favor of *myocd-A* (see Fig. 3D) may have maladaptive consequences for LV functioning.

An additional influence that might act to impair systolic performance is that under our experimental conditions the target tissue to be transfected by the *myocd-A* DNA was not only proper LV myocardium but also its outer-most layer including the coronary arteriolar network. In this context, MYOCD overexpression in human vascular SMCs induced a hypercontractile phenotype by enhancing the expression of SRF/MYOCD-dependent contractile genes (Chow *et al.*, 2007). In this work, we detected the up-regulation of several SMC-specific contractile filament genes (especially*, tagln/SM22*) in response to *myocd-A* delivery (see Table 3, Fig. 5B). Therefore, it is not unreasonable to speculate that a possible "contaminant" *myocd-A* overexpression in both superficial and intramyocardial arteriolar network could promote a hypercontractile SMC phenotype in LV microvasculature, which, in turn, might result in disturbance of LV myocardium perfusion and contractile performance. At present, we have no direct experimental results supporting this hypothesis, and only further work will clarify whether such mechanism is really operating.

Forced *myocd* expression in cultured neonatal ventricular cardiomyocytes resulted in cell hypertrophy and induction of endogenous *anf* transcription (Badorff *et al.*, 2005; Xing *et al.*, 2006). In this work, neither histological signs of ectopic cardiomyocyte hypertrophy nor appreciable *anf* gene up-regulation were observed in target LVFW regions two days after *myocd-A* gene delivery. Most probably, this is because LV-cardiomyocytes in 6-8-day-old piglets undergo intensive physiological hypertrophy that is accompanied by a relatively high ventricular *anf* expression (M. Torrado and A.T. Mikhailov, unpublished data).

Such a hypertrophic state of targeting LV-cardiomyocytes may mask or even impose a pro-hypertrophic effect of forced *myocd* expression *in vivo.* Alternately, the *myocd*-mediated hypertrophic effect, which has been identified in an *in vitro* model system, may be difficult to mimic in *in vivo* settings because the response of targeting LV-cardiomyocytes to elevated *myocd* expression *in vivo* could be modified by their interactions with adjacent non-transfected working myocytes as well as with other cell types (i.e., impulse-conducting cardiomyocytes, endothelial cells, and cardiac fibroblasts) compounding neonatal LV-tissue.

In summary, our data revealed that under apparently normal hypertrophic growth the outcome of the response of the LV, as a heterotypic cell system, to elevated *myocd-A* expression might be maladaptive. More broadly, this observation is consistent with the suggestion (Pipes *et al.*, 2006) that *myocd* overexpression might represent a maladaptive response to pathological remodeling of the heart.

Concluding remarks

This study is the first to show possible functional consequences of forced MYOCD-A production in the LVFW resulting from direct intra-myocardial gene transfer *in vivo*. Despite the efficiency of our gene delivery technique, it is unrealistic to expect a 100% *myocd-A*-transfection of every cell in LVFW. Nevertheless, ventricular performance was affected in experimental piglets although, on average, no more than 40% of the LVFW was efficiently transfected by *myocd-A*. The results show that even local changes in MYOCD dosage (and, consequently, in MYOCD-A/MYOCD-B ratio) may modulate the responsiveness of LV-myocardium to overload during early postnatal development. Observed transient deterioration in ventricular performance of the neonatal heart in response to a local *myocd-A* overexpression in the LV myocardium suggests that cessation of ventricular *myocd-A* expression at early-stage cardiomyopathy might represent a safety feature from a therapeutic point of view. Although this is an encouraging idea, it remains to be determined whether *myocd-A* forced expression in the LV may be a maladaptive background upon stress, resulting in pathological LV remodeling. Our preliminary results indicate that in neonatal piglets LV *myocd-A* transfection followed by adriamycin-induced cardiomyopathy resulted in a significantly lower survival rate of the transfected animals compared to controls.

Materials and Methods

Gene cloning and in vitro *expression*

The full-length porcine *myocd-A* (GenBank accession no. NM_213745) and *myocd-B* (this work, see Fig. 2A) were amplified from piglet LV oligo-dT primed cDNA, cloned into T7 promoter-containing vector pcDNA3.1/*myc*-His B (Invitrogen), verified by sequencing and expressed *in vitro* using TnT T7 Quick Coupled *in vitro* Transcription/Translation (IVTT) System (Promega) in the presence or absence of [^{35}S]-labeled methionine as described (Torrado *et al.*, 2005a). The corresponding protein products were purified on Sephadex G-50 columns (Amersham Bioscience) and used in downstream SDS-PAGE and Western-blot experiments.

Plasmid DNA

The following expression plasmids in p3XFLAG-CMV-14 vector (Sigma) driven by a human cytomegalovirus (CMV) promoter/enhancer were used: (1) *myocd-A* plasmid, encoding a FLAG-tagged full-length porcine *myocd-A* gene; (2*) hop* plasmid, encoding a FLAG-tagged full-length porcine *hop* (GenBank accession no. NM_213792), (3) reporter plasmid encoding the bacterial gene for β–galactosidase (*β-gal*), and (4) vector plasmid only (control empty vector). All the DNA constructs were verified by sequencing. Plasmids grown in XL1-Blue Supercompetent *E. coli* cells (Stratagene) were purified by using a PureLink HiPure plasmid filter purification kit (Invitrogen) according to the manufacturer's protocol. Plasmids were formulated at a final DNA concentration of 1 mg/ml in sterile isotonic saline (PBS).

Animals and experimental procedures

Animal care and handling conformed to the guidelines of the European Commission Directive 86/609/EEC on the protection of animals used for experimental and other scientific purposes and were approved by the Institutional Ethics Committee of the University of La Coruña. Litters of Large White domestic pigs were maintained in the Nütinger automatic nursery system, randomized in five groups and assigned to receive intramyocardial injections of: (1) *myocd-A* plasmid DNA (n=16), (2) *hop*-plasmid DNA (n=6), (3) β–gal-plasmid DNA (n=6), (4) vector alone plasmid (n=8), and (5) 2% Indian ink (Winsor & Newton, UK) suspension in PBS (n=6). Neonatal 6-day-old piglets were sedated, intubated, and anesthetized. While under anesthesia and mechanical ventilatory support, ECG was monitored followed by trans-costotranversal inserting a fiber-optic catheter (Cardio-Optics Inc.) and endoscopic tubular (3 mm) cannula into left chest cavity. The pericardium was opened, and the catheter and cannula were moved to access and visualize the ventral surface of the left ventricle free wall (LVFW). Then, the endoscopic needle was introduced into the cannula, and intramyocardial injections were performed (as detailed in the body text) in the ventro-lateral area of the LVFW. To minimize leakage of injectate from the puncture site, each injection was performed slowly under direct visualization. Intra-operative monitoring of cardiovascular parameters (blood pressure, pulse rate, body temperature) was performed during the procedure. On the 2nd and 7th day after gene transfer, ECG was monitored in closed-chest piglets followed by measurements of ventricular end-systolic (LV/RV-ESP) and end-diastolic pressure (LV/RV-EDP) in open-chest piglets using a Dräger UM3.1 pressure transducer and a recording device (Drägerwerk AG, Germany) as described (Torrado *et al.*, 2006). Then animals were euthanized and the hearts were rapidly excised, weighed, and photographed. All these procedures were conducted by two investigators blinded to the experimental design. The ventral LVFW of each heart was sectioned into 9 regions (~ 1x1 cm each; see Fig. 3) which were then assayed individually for RNA and protein isolation, and tissue fixation (Torrado *et al.*, 2004; Torrado *et al.*, 2005b; Torrado *et al.*, 2006).

Semiquantitative RT-PCR

Total RNA was extracted by RNAeasy-Mini Kit (Qiagen) according to the manufacturer's protocol, subjected to on column digestion of DNA with RNase-free DNase (Qiagen), and reverse transcribed using the SuperScript III (Invitrogen) and oligo-dT primers. Semiquantitative RT-PCR was performed as described previously (Torrado *et al.*, 2003; Torrado *et al.*, 2004). All PCR reactions included primers for the candidate (*myocd-A* or *myocd-B*) and control (ribosomal protein L19 - RPL19) genes. Porcine *myocd-A* and *myocd-B* were amplified with the oligonucleotides 273 and 270 generating 294-bp *myocd-A* and 438-bp *myocd-B* PCR-products (see Fig. 2A,B). Discriminating primer set for the specific amplification of delivered FLAG-tagged *myocd-A* was 279 and 239 (derived from the FLAG vector sequence) for a 577-bp PCR product. The porcine *RPL19* (accession no: BI181894) was used to design oligonucleotides 36 and 65 for a 480-bp PCR product. Reactions, including NRT (non-RT control) and NTC (no template control), were performed at least in triplicate. PCR products were visualized on 2% agarose gels by ethidium bromide (EtBr) staining and band intensity was estimated by densitometry (VersaDoc 1000) and Quantity One software (Bio-Rad).

Quantitative real-time RT-PCR (qRT-PCR)

qRT-PCR was performed using SYBR Green Master Mix (Bio-Rad) on

Bio-Rad IQ5 instrument as described (Torrado *et al.*, 2006) with the addition of primer pairs targeting transcripts encoding (see Table 3) the porcine *mlc3f* (primers 292 and 293), *anf* (primers 266 and 267), *cnn1* (primers 295 and 296), *tagln/SM-22* (primers 297 and 298), and *actg2* (primers 301 and 302). The primer pairs were located in different exons to rule out genomic DNA amplification. Each primer pair used yielded a single peak of dissociation on the melting curve and a single band with the expected size on agarose gel. Identity of the PCR products was confirmed by sequencing. Non-template and non-RT RNA template reactions were used as negative controls. Results were normalized against *RPL19* expression (oligonucleotides 64 and 206). The efficiency of target and reference amplification was tested to be approximately equal. Primer sequences and additional details on RT-PCR/qRT-PCR are available upon request.

β-gal enzyme activity assay

β-gal enzyme activity was measured in LVFW extracts using a high sensitivity β- galactosidase Assay Kit (Stratagene) with standards supplied by the manufacturer at pH 8.0 to minimize non-specific staining. Enzyme activity values were normalized to total protein concentration determined using the Bio-Rad *DC* Protein Assay.

Antibody production

The C-terminal part (amino acid residues 731-873; CT-MYOCD) of porcine MYOCD-A (GenBank accession no: NP_998910) was cloned into pCAL-n-FLAG vector (Stratagene) and expressed in Rosetta-gami B(DE3) (Novagen). Recombinant CT-MYOCD-A (fused to the 5-kDa tag, which included the calmodulin-binding peptide (CBP) and FLAG peptide) was purified from bacterial lysates using calmodulin-affinity resin (Stratagene) and used as immunogen. Polyclonal antibodies against porcine CT-MYOCD-A were raised in rabbits by Davids Biotechnologie (Regenburg, Germany). Obtained anti-CT-MYOCD-A antibodies (marked by us as AB531) were shown to be specific for recombinant porcine MYOCD-A and MYOCD-B by Western blot with competing peptide. Five fragments covering the major part of the sequence of porcine *myocd-A* were cloned and expressed as just described, and resulting purified products were probed by Western blot with anti-FLAG (Sigma) and our lab-derived AB531 antibodies (Fig. 4B,C). Anti-FLAG antibodies detected each of the expressed *myocd-A* fragments, whereas AB531 antibodies recognized only the CT-MYOCD-A (i.e., the immunogen); no cross-reactivity was observed with other MYOCD-A-derived fragments. These results indicated that AB531 antibodies detect only the TAD-containing CT-fragment, a region that is similar for all the *myocd* isoforms identified to date in cardiac and SMC-containing tissues (see Fig. 4A).

SDS-PAGE and Western blotting

LVFW tissue samples were homogenized and solubilized in standard 2x Laemmli sample buffer as previously described (Torrado *et al.*, 2006). Extracted proteins were subjected to SDS-PAGE (Mini-Protean-III, Bio-Rad), stained with Coomassie or blotted onto PVDF membranes (Hybond-P, Amersham Bioscience), and probed with rabbit polyclonal antibodies against porcine MYOCD or mouse monoclonal anti-my*c* or anti-FLAG antibodies (Sigma). Molecular weight (MW) standards (MARK-12 and SeeBlue Plus2 from Invitrogen, and high and low MW calibration kits from Amersham Biosciences) were included on each gel. Equivalence of protein loading was confirmed by Amido-Black staining of blots before (blot-replicas) and after immunodetection. Blocking, washing, incubation with diluted primary and secondary HRP-conjugated antibodies (Sigma), and visualization of immunodecorated bands by the Super-Signal West Pico chemiluminescent substrate (Pierce Biotechnology) was carried out as previously described (Torrado *et al.*, 2005a; Torrado *et al.*, 2006). IVTT-synthesized *myc*-tagged pig MYOCD-A or MYOCD-B was included as a positive control for anti-CT-MYOCD-A antibodies. Substitution of the primary antibodies with anti-CT-MYOCD-A antibodies neutralized by the competing peptide was included in negative controls.

Histology

LVFW tissue samples were fixed in 4% formalin in PBS and embedded in paraplast (Sigma). Serial transverse 5 μm-sections were subjected to haematoxylin-eosin, Masson's trichrome and von Kossa staining (Bancroft and Stevens, 1996) and examined under a "Nikon Eclipse 600" microscope by an experienced technician blinded to the gene-delivery experiments.

Statistics

Results are expressed as mean± SEM. Statistical significance was evaluated by Student's *t* test. Statistical analyses were performed with the SPSS 13 software. A value of $p< 0.05$ was considered statistically significant.

Acknowledgements

We thank Professor Juan Aréchaga for the invitation to contribute an article for this issue. This work was supported by a Grant (SAF2004-01462) from Spanish Ministry of Education and Science and by a Grant (PGIDIT04BTF16001 PR5) from the Autonomic Government of Galicia.

References

BADORFF, C., SEEGER, F.H., ZEIHER, A.M. and DIMMELER, S. (2005). Glycogen synthase kinase 3beta inhibits myocardin-dependent transcription and hypertrophy induction through site-specific phosphorylation. *Circ Res* 97: 645-654.

BANCROFT, J.D. and STEVENS, A. (1996). *Theory and practice of histological techniques*. Churchill Livingstone, Edinburgh.

CALLIS, T.E., CAO, D. and WANG, D.Z. (2005). Bone morphogenetic protein signaling modulates myocardin transactivation of cardiac genes. *Circ Res* 97: 992-1000.

CHEN, F., KOOK, H., MILEWSKI, R., GITLER, A.D., LU, M.M., LI, J., NAZARIAN, R., SCHNEPP, R., JEN, K., BIBEN, C., RUNKE, G., MACKAY, J.P., NOVOTNY, J., SCHWARTZ, R.J., HARVEY, R.P., MULLINS, M.C. and EPSTEIN, J.A. (2002a). Hop is an unusual homeobox gene that modulates cardiac development. *Cell* 110: 713-723.

CHEN, J., KITCHEN, C.M., STREB, J.W. and MIANO, J.M. (2002b). Myocardin: a component of a molecular switch for smooth muscle differentiation. *J Mol Cell Cardiol* 34: 1345-1356.

CHOW, N., BELL, R.D., DEANE, R., STREB, J.W., CHEN, J., BROOKS, A., VAN NOSTRAND, W., MIANO, J.M. and ZLOKOVIC, B.V. (2007). Serum response factor and myocardin mediate arterial hypercontractility and cerebral blood flow dysregulation in Alzheimer's phenotype. *Proc Natl Acad Sci USA* 104: 823-828.

CREEMERS, E.E., SUTHERLAND, L.B., MCANALLY, J., RICHARDSON, J.A. and OLSON, E.N. (2006a). Myocardin is a direct transcriptional target of Mef2, Tead and Foxo proteins during cardiovascular development. *Development* 133: 4245-4256.

CREEMERS, E.E., SUTHERLAND, L.B., OH, J., BARBOSA, A.C. and OLSON, E.N. (2006b). Coactivation of MEF2 by the SAP domain proteins myocardin and MASTR. *Mol Cell* 23: 83-96.

DU, K.L., IP, H.S., LI, J., CHEN, M., DANDRE, F., YU, W., LU, M.M., OWENS, G.K. and PARMACEK, M.S. (2003). Myocardin is a critical serum response factor cofactor in the transcriptional program regulating smooth muscle cell differentiation. *Mol Cell Biol* 23: 2425-2437.

ELORANTA, J.J. and HURST, H.C. (2002). Transcription factor AP-2 interacts with the SUMO-conjugating enzyme UBC9 and is sumolated in vivo. *J Biol Chem* 277: 30798-30804.

HENDRIX, J.A., WAMHOFF, B.R., MCDONALD, O.G., SINHA, S., YOSHIDA, T. and OWENS, G.K. (2005). 5' CArG degeneracy in smooth muscle alpha-actin is required for injury-induced gene suppression in vivo. *J Clin Invest* 115: 418-427.

KELLY, R., ALONSO, S., TAJBAKHSH, S., COSSU, G. and BUCKINGHAM, M. (1995). Myosin light chain 3F regulatory sequences confer regionalized cardiac and skeletal muscle expression in transgenic mice. *J Cell Biol* 129: 383-396.

KELLY, R.G., ZAMMIT, P.S., SCHNEIDER, A., ALONSO, S., BIBEN, C. and BUCKINGHAM, M.E. (1997). Embryonic and fetal myogenic programs act

through separate enhancers at the MLC1F/3F locus. *Dev Biol* 187: 183-199.

KOOK, H. and EPSTEIN, J.A. (2003). Hopping to the beat. Hop regulation of cardiac gene expression. *Trends Cardiovasc Med* 13: 261-264.

LI, H.J., HAQUE, Z., LU, Q., LI, L., KARAS, R. and MENDELSOHN, M. (2007). Steroid receptor coactivator 3 is a coactivator for myocardin, the regulator of smooth muscle transcription and differentiation. *Proc Natl Acad Sci USA* 104: 4065-4070.

LI, S., WANG, D.Z., WANG, Z., RICHARDSON, J.A. and OLSON, E.N. (2003). The serum response factor coactivator myocardin is required for vascular smooth muscle development. *Proc Natl Acad Sci USA* 100: 9366-9370.

LIU, N. and OLSON, E.N. (2006). Coactivator control of cardiovascular growth and remodeling. *Curr Opin Cell Biol* 18: 715-722.

LONG, X., CREEMERS, E.E., WANG, D.Z., OLSON, E.N. and MIANO, J.M. (2007). Myocardin is a bifunctional switch for smooth versus skeletal muscle differentiation. *Proc Natl Acad Sci USA* 104: 16570-16575.

MCGREW, M.J., BOGDANOVA, N., HASEGAWA, K., HUGHES, S.H., KITSIS, R.N. and ROSENTHAL, N. (1996). Distinct gene expression patterns in skeletal and cardiac muscle are dependent on common regulatory sequences in the MLC1/3 locus. *Mol Cell Biol* 16: 4524-4534.

MICHAEL, A., HAQ, S., CHEN, X., HSICH, E., CUI, L., WALTERS, B., SHAO, Z., BHATTACHARYA, K., KILTER, H., HUGGINS, G., ANDREUCCI, M., PERIASAMY, M., SOLOMON, R.N., LIAO, R., PATTEN, R., MOLKENTIN, J.D. and FORCE, T. (2004). Glycogen synthase kinase-3beta regulates growth, calcium homeostasis, and diastolic function in the heart. *J Biol Chem* 279: 21383-21393.

MULLER-BORER, B.J., CASCIO, W.E., ESCH, G.L., KIM, H.S., COLEMAN, W.B., GRISHAM, J.W., ANDERSON, P.A. and MALOUF, N.N. (2007). Mechanisms controlling the acquisition of a cardiac phenotype by liver stem cells. *Proc Natl Acad Sci USA* 104: 3877-3882.

OH, J., WANG, Z., WANG, D.Z., LIEN, C.L., XING, W. and OLSON, E.N. (2004). Target gene-specific modulation of myocardin activity by GATA transcription factors. *Mol Cell Biol* 24: 8519-8528.

OKA, T., XU, J. and MOLKENTIN, J.D. (2007). Re-employment of developmental transcription factors in adult heart disease. *Semin Cell Dev Biol* 18: 117-131.

OLSON, E.N. (2004). A decade of discoveries in cardiac biology. *Nat Med* 10: 467-474.

PARLAKIAN, A., CHARVET, C., ESCOUBET, B., MERICSKAY, M., MOLKENTIN, J.D., GARY-BOBO, G., DE WINDT, L.J., LUDOSKY, M.A., PAULIN, D., DAEGELEN, D., TUIL, D. and LI, Z. (2005). Temporally controlled onset of dilated cardiomyopathy through disruption of the SRF gene in adult heart. *Circulation* 112: 2930-2939.

PARMACEK, M.S. (2007). Myocardin-related transcription factors: critical coactivators regulating cardiovascular development and adaptation. *Circ Res* 100: 633-644.

PIPES, G.C., CREEMERS, E.E. and OLSON, E.N. (2006). The myocardin family of transcriptional coactivators: versatile regulators of cell growth, migration, and myogenesis. *Genes Dev* 20: 1545-1556.

PIPES, G.C., SINHA, S., QI, X., ZHU, C.H., GALLARDO, T.D., SHELTON, J., CREEMERS, E.E., SUTHERLAND, L., RICHARDSON, J.A., GARRY, D.J., WRIGHT, W.E., OWENS, G.K. and OLSON, E.N. (2005). Stem cells and their derivatives can bypass the requirement of myocardin for smooth muscle gene expression. *Dev Biol* 288: 502-513.

QIU, P., RITCHIE, R.P., FU, Z., CAO, D., CUMMING, J., MIANO, J.M., WANG, D.Z., LI, H.J. and LI, L. (2005). Myocardin enhances Smad3-mediated transforming growth factor-beta1 signaling in a CArG box-independent manner: Smad-binding element is an important cis element for SM22alpha transcription in vivo. *Circ Res* 97: 983-991.

SAPETSCHNIG, A., RISCHITOR, G., BRAUN, H., DOLL, A., SCHERGAUT, M., MELCHIOR, F. and SUSKE, G. (2002). Transcription factor Sp3 is silenced through SUMO modification by PIAS1. *EMBO J* 21: 5206-5215.

SHIN, C.H., LIU, Z.P., PASSIER, R., ZHANG, C.L., WANG, D.Z., HARRIS, T.M., YAMAGISHI, H., RICHARDSON, J.A., CHILDS, G. and OLSON, E.N. (2002). Modulation of cardiac growth and development by HOP, an unusual homeodomain protein. *Cell* 110: 725-735.

SMALL, E.M., WARKMAN, A.S., WANG, D.Z., SUTHERLAND, L.B., OLSON, E.N. and KRIEG, P.A. (2005). Myocardin is sufficient and necessary for cardiac gene expression in *Xenopus*. *Development* 132: 987-997.

TORRADO, M., LOPEZ, E., CENTENO, A., CASTRO-BEIRAS, A. and MIKHAILOV, A.T. (2004). Left-right asymmetric ventricular expression of CARP in the piglet heart: regional response to experimental heart failure. *Eur J Heart Fail* 6: 161-172.

TORRADO, M., LOPEZ, E., CENTENO, A., MEDRANO, C., CASTRO-BEIRAS, A. and MIKHAILOV, A.T. (2003). Myocardin mRNA is augmented in the failing myocardium: expression profiling in the porcine model and human dilated cardiomyopathy. *J Mol Med* 81: 566-577.

TORRADO, M., NESPEREIRA, B., BOUZAMAYOR, Y., CENTENO, A., LOPEZ, E. and MIKHAILOV, A.T. (2006). Differential atrial versus ventricular ANKRD1 gene expression is oppositely regulated at diastolic heart failure. *FEBS Lett* 580: 4182-4187.

TORRADO, M., NESPEREIRA, B. and MIKHAILOV, A.T. (2005a). Fetal cardiac control genes: implications for postnatal heart growth and heart disease. *Trends Dev Biol* 1: 27-38.

TORRADO, M., NESPEREIRA, B., LOPEZ, E., CENTENO, A., CASTRO-BEIRAS, A. and MIKHAILOV, A.T. (2005b). ANKRD1 specifically binds CASQ2 in heart extracts and both proteins are co-enriched in piglet cardiac Purkinje cells. *J Mol Cell Cardiol* 38: 353-365.

VAN TUYN, J., ATSMA, D.E., WINTER, E.M., VAN DER VELDE-VAN DIJKE, I., PIJNAPPELS, D.A., BAX, N.A., KNAAN-SHANZER, S., GITTENBERGER-DE GROOT, A.C., POELMANN, R.E., VAN DER LAARSE, A., VAN DER WALL, E.E., SCHALIJ, M.J. and DE VRIES, A.A. (2007a). Epicardial cells of human adults can undergo an epithelial-to-mesenchymal transition and obtain characteristics of smooth muscle cells in vitro. *Stem Cells* 25: 271-278.

VAN TUYN, J., PIJNAPPELS, D.A., DE VRIES, A.A.F., DE VRIES, I., VAN DER VELDE-VAN DIJKE, I., KNAAN-SHANZER, S., VAN DER LAARSE, A., SCHALIJ, M.J. and ATSMA, D.E. (2007b). Fibroblasts from human postmyocardial infarction scars acquire properties of cardiomyocytes after transduction with a recombinant myocardin gene. *FASEB J* 21: 3369-3379.

VAN TUYN, J., KNAAN-SHANZER, S., VAN DE WATERING, M.J., DE GRAAF, M., VAN DER LAARSE, A., SCHALIJ, M.J., VAN DER WALL, E.E., DE VRIES, A.A. and ATSMA, D.E. (2005). Activation of cardiac and smooth muscle-specific genes in primary human cells after forced expression of human myocardin. *Cardiovasc Res* 67: 245-255.

WANG, D., CHANG, P.S., WANG, Z., SUTHERLAND, L., RICHARDSON, J.A., SMALL, E., KRIEG, P.A. and OLSON, E.N. (2001). Activation of cardiac gene expression by myocardin, a transcriptional cofactor for serum response factor. *Cell* 105: 851-862.

WANG, D.Z., LI, S., HOCKEMEYER, D., SUTHERLAND, L., WANG, Z., SCHRATT, G., RICHARDSON, J.A., NORDHEIM, A. and OLSON, E.N. (2002). Potentiation of serum response factor activity by a family of myocardin-related transcription factors. *Proc Natl Acad Sci USA* 99: 14855-14860.

WANG, J., LI, A., WANG, Z., FENG, X., OLSON, E.N. and SCHWARTZ, R.J. (2007). Myocardin sumoylation transactivates cardiogenic genes in pluripotent 10T1/2 fibroblasts. *Mol Cell Biol* 27: 622-632.

WANG, Z., WANG, D.Z., HOCKEMEYER, D., MCANALLY, J., NORDHEIM, A. and OLSON, E.N. (2004). Myocardin and ternary complex factors compete for SRF to control smooth muscle gene expression. *Nature* 428:185-189.

WANG, Z., WANG, D.Z., PIPES, G.C. and OLSON, E.N. (2003). Myocardin is a master regulator of smooth muscle gene expression. *Proc Natl Acad Sci USA* 100: 7129-7134.

XING, W., ZHANG, T.C., CAO, D., WANG, Z., ANTOS, C.L., LI, S., WANG, Y., OLSON, E.N. and WANG, D.Z. (2006). Myocardin induces cardiomyocyte hypertrophy. *Circ Res* 98: 1089-1097.

YOSHIDA, T., KAWAI-KOWASE, K. and OWENS, G.K. (2004). Forced expression of myocardin is not sufficient for induction of smooth muscle differentiation in multipotential embryonic cells. *Arterioscler Thromb Vasc Biol* 24: 1596-1601.

YOSHIDA, T., SINHA, S., DANDRE, F., WAMHOFF, B.R., HOOFNAGLE, M.H., KREMER, B.E., WANG, D.Z., OLSON, E.N. and OWENS, G.K. (2003). Myocardin is a key regulator of carg-dependent transcription of multiple smooth muscle marker genes. *Circ Res* 92: 856-865.

ZHANG, X., AZHAR, G., ZHONG, Y. and WEI, J.Y. (2004). Identification of a novel serum response factor cofactor in cardiac gene regulation. *J Biol Chem* 279: 55626-55632.

Related, previously published *Int. J. Dev. Biol.* articles

See our recent Special Issue ***Ear Development*** edited by Fernando Giraldez and Bernd Fritzsch at: http://www.ijdb.ehu.es/web/contents.php?vol=51&issue=6-7

See our Special Issue ***Mammalian Reproduction & Development*** in honor of Anne McLaren and edited by Brigid Hogan at: http://www.ijdb.ehu.es/web/contents.php?vol=45&issue=3

Myoskeletin, a factor related to Myocardin, is expressed in somites and required for hypaxial muscle formation in Xenopus
Hui Zhao, Martha L. Rebbert and Igor B. Dawid
Int. J. Dev. Biol. (2007) 51: 315-320

Heart formation and left-right asymmetry in separated right and left embryos of a newt
Kazuhiro Takano, Yuzuru Ito, Shuichi Obata, Tsutomu Oinuma, Shinji Komazaki, Hiroaki Nakamura and Makoto Asashima
Int. J. Dev. Biol. (2007) 51: 265-272

Thyroid hormone receptor expression in the obligatory paedomorphic salamander Necturus maculosus
Virginie Vlaeminck-Guillem, Rachid Safi, Philippe Guillem, Emmanuelle Leteurtre, Martine Duterque-Coquillaud and Vincent Laudet
Int. J. Dev. Biol. (2006) 50: 553-560

Biophysical mechanisms of cardiac looping
Larry A. Taber
Int. J. Dev. Biol. (2006) 50: 323-332

Biophysical regulation during cardiac development and application to tissue engineering
Sharon Gerecht-Nir, Milica Radisic, Hyoungshin Park, Christopher Cannizzaro, Jan Boublik, Robert Langer and Gordana Vunjak-Novakovic
Int. J. Dev. Biol. (2006) 50: 233-243

The cap 'n' collar family member NF-E2-related factor 3 (Nrf3) is expressed in mesodermal derivatives of the avian embryo
Heather C. Etchevers
Int. J. Dev. Biol. (2005) 49: 363-367

Amphibian in vitro heart induction: a simple and reliable model for the study of vertebrate cardiac development
Takashi Ariizumi, Masayoshi Kinoshita, Chika Yokota, Kazuhiro Takano, Keiichi Fukuda, Nobuo Moriyama, George M Malacinski and Makoto Asashima
Int. J. Dev. Biol. (2003) 47: 405-410

Induction and patterning of the cardiac conduction system
David J Pennisi, Stacey Rentschler, Robert G Gourdie, Glenn I Fishman and Takashi Mikawa
Int. J. Dev. Biol. (2002) 46: 765-775

Efficient Cre-mediated deletion in cardiac progenitor cells conferred by a 3'UTR-ires-Cre allele of the homeobox gene Nkx2-5
Edouard G Stanley, Christine Biben, Andrew Elefanty, Louise Barnett, Frank Koentgen, Lorraine Robb and Richard P Harvey
Int. J. Dev. Biol. (2002) 46: 431-439

Heat shock factor 2 is activated during mouse heart development
M Eriksson, E Jokinen, L Sistonen and S Leppä
Int. J. Dev. Biol. (2000) 44: 471-477

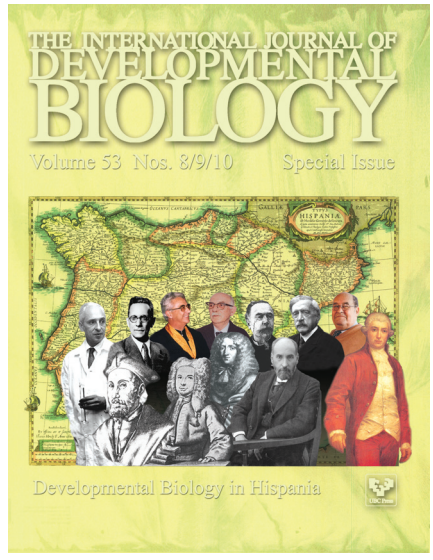

5 yr ISI Impact Factor (2008) = 3.271